SPE 166077

Large Scale Jet Pump Performance Optimization in a Viscous Oil Field

Manjit K. Singh, Dhruva Prasad, Aditya K. Singh, Mihir Jha, and Rohit Tandon SPE, Cairn India Ltd

Copyright 2013, Society of Petroleum Engineers

This paper was prepared for presentation at the SPE Annual Technical Conference and Exhibition held in New Orleans, Louisiana, USA, 30 September–2 October 2013.

This paper was selected for presentation by an SPE program committee following review of information contained in an abstract submitted by the author(s). Contents of the paper have not been reviewed by the Society of Petroleum Engineers and are subject to correction by the author(s). The material does not necessarily reflect any position of the Society of Petroleum Engineers, its officers, or members. Electronic reproduction, distribution, or storage of any part of this paper without the written consent of the Society of Petroleum Engineers is prohibited. Permission to reproduce in print is restricted to an abstract of not more than 300 words; illustrations may not be copied. The abstract must contain conspicuous acknowledgment of SPE copyright.

Abstract

This paper discusses the performance monitoring and optimization of large scale jet pumping in Mangala field, one of the biggest onshore fields in India. Mangala field is characterized by multi-Darcy sandstones, containing waxy and viscous crude oil. Currently, the field is producing at plateau of 150,000 BOPD.

The base development plan for the field included hot water flooding; this also makes water heated up to 80 °C available at the well pads as power fluid for jet pumping. Jet pump was selected as the preferred artificial lift method in deviated wells, as it addresses all flow assurance issues arising due to high wax appearance temperature of Mangala crude.

Jet pumps provide the required drawdown for sustained liquid production both at low and high water cut. With significant number of wells operating on jet pump, it has become crucial to monitor the performance and optimize for maximum efficiency application by varying operating parameters, changing the nozzle throat combinations and making other adjustments. Currently, Cairn is monitoring the real time jet pump operating parameters on a daily basis by virtue of DOF (Digital Oil Field). DOF has not only eased the tedious task of jet pump monitoring in bulk but also has reduced the response time to any failures/damage in the pump. Liquid handling capacity of the processing plant has become crucial with increasing field water cut and more jet pump installations. Jet pump performance optimization for maximum efficiency has now started to play an important role in not only reducing the burden of the processing facility but also in improving the production profile of the wells.

This paper will discuss the use of a methodology based on an in-house developed algorithm for monitoring the efficiency of the pumps, with supporting field examples. This paper will also make an attempt to analyze the effect of different operating conditions on the pump performance curves published in the literature.

Introduction

The onshore Mangala field is located in the north-west part of India in the Barmer Basin (Fig.1). The field was discovered in January 2004. The main reservoir unit in Mangala field is the Fatehgarh group, which is a very high quality quartzose sandstone reservoir, with high net to gross, high porosity (21-28%) and high permeability (200 mD to 20,000 mD). The oil is waxy and viscous (~18cP), with wax appearance temperatures (60°C) close to reservoir temperature (65°C).

The Mangala field has been developed with a more than 150 wells with dedicated producers and injectors for each Fatehgarh sand member. Electric Submersible Pump (ESP) and Jet Pump (JP) are the twomain artificial lift mechanisms in the field with significant number of wells currently flowing on JP. The field is producing ~ 150,000 BOPD. Fig 2 shows the contribution of production from different artificial lift mechanisms in the field.

Reverse flow JP were selected for field application with hot water as power fluid (PF) is pumped into the casing– tubing annulus, and the combined formation and power fluid mixture is produced from the tubing (Fig.3).(Chavan et al.). The main reasons for selection of JP in deviated producers were:

- Provide down-hole flow assurance by utilizing hot water power fluid already available at well pads for surface flow assurance and hot water flooding in the reservoir
- Ability to lift a wide range of liquid rates expected from Mangala (500 – 8,000 BLPD)
- Low workover frequency and ease of installation/retrieval by wire line
- Relatively simple to operate with no moving parts
- Good tolerance to sand production

Table 1 shows the typical operating range of the jet pumps and the reservoir and fluid parameters in the field.

Full Field Implementation and Learnings

Mangala field production started in August 2009. To gain the early experience of JP operation, a field trial was conducted in 2010 and the objectives in terms of providing drawdown and operability were achieved. After the field trial, JPs were installed in the wells as and when requiredwith the following objectives:

- Restore liquid production in case of increase in water cut
- Increase liquid production by means of providing higher drawdown
- Cleanup wells by installing JP, in case heavy gradients were observed in well during startup
- Temporarily install JP in horizontal wells where the ESP was under troubleshooting or failed

The initial design philosophy was to use 0.7 barrels of power fluid for every barrel of liquid produced. JP sizing was done thru modeling and installed per design in the field. Given the number of wells requiring jet pumps, which were all installed at similar depths, with similar operating conditions and power fluid pressures, the optimum PF rate was established for different nozzle sizes. This helped to quickly verify the PF rate required for newly installed JP. If variationwas observed in expected vsactual performance, then detailed checks of the PF meter calibration, well condition, inflow/outflow model, and other variables were done. The following parameters and observations were estabilished in based on all the jet pump data:

- Desired drawdown can be provided and controlled by varying the power fluid inlet pressure and the wellhead choke (Fig. 4 & 5)
- The amount of power fluid required for different JP nozzle size at maximum operating surface pressures was established
- It was concluded that at constant throat size, PF rate is significantly affected by varying the nozzle size. Whereas throat size variation had little effect on the PF rate for a given nozzle size. Varying THP also had little impact on PF rate for a particular nozzle/throat combination
- In some wells even by lowering THP, no increase in liquid production rate was observed although commercial softwares suggested otherwise. This was mainly attributed to choked flow in the JP, which is explained in detail later in the paper
- The average power fluid to produced fluid ratio was maintained at approx. 0.7

Surveillance

The JP monitoring and performance optimization was facilitated by the DOF application. All the wells, headers, and processing facilities are equipped with the pressure, temperature, flow rate, and status sensors at critical locations. The data

from the multiphase flow meters (MPFM), permanent downhole gauges (PDG) and other equipment is also available digitally. End to end workflows were developed to process the large amounts of streaming data, enabling the monitoring of individual wells and processes.

Because of the significant number of wells, it was very challenging to monitor the individual JP and well performance. Therefore, a customized JP analysis page was developed on the DOF interface, wherein real time data from the sensors for all the JP wells were tabulated and calculation of important parameters was done in real time (Fig. 6). This page proved extremely helpful in the day-to-day monitoring and troubleshooting of the JP wells. It has enabled detection of problems and variances almost instantly and has enabled the team to diagnose and troubleshoot, thereby reducing the response time and increasing well uptime.

The expected power fluid (PF) rate for a given well is derived from the industry standard nodal analysis software using prevailing operating conditions and reservoir parameters. Post JP installation, the variance of the actual versus predicted PF rate is calculated and displayed on the page. This variance is the most important parameter for monitoring because all other parameters like PF pressure, header pressure, etc. generally remain constant. If the variance is more than 20%, then the first step is to recalibrate the flow transmitter (FT). If the variance doesn't improve post FT recalibration, the next step is to check the JP installation date. In the case of a very recent JP installation, the JP model is again recalibrated. For older JP installations, the trending of the wellhead parameters is then done. The trend of decline in the PF rate can indicate the mechanism of JP damage. If the drop is sudden then, it is probably due to the mechanical failure of the pump and if the fall is gradual over time, it is more likely to be scaling of the JP nozzle. If the PF rate increases suddenly, then it can be a case of packer failure. The latest well test data also helps to identify issues with the jet pump. If the reservoir fluid rate has declined significantly since JP installation but the PF rate remains nearly constant, then it may indicate the scaling of the throat and diffuser as opposed to a PI decline.

Wellhead temperature (WHT) is also a very important parameter in the monitoring of well performance. The Power Fluid temperature is maintained between 75°C - 80°C while the reservoir temperature is ~60°C. It has been observed that for the Mangala wells, the optimum operating WHT is between 60-70^{0}C for the operating producing fluid to power fluid ratio (1.0 – 1.5). For a WHT lower than 60^{0}C, either the well most likely produces with high gas oil ratio (GOR) or the PF is getting injected in to the formation or the nozzle might be plugged. On the other hand, if the WHT is more than 70^{0}C, either the well has a very high WC or only the PF is getting circulated. These possibilities are checked through the well tests and observing the other parameters like PF rate, PF pressure and the well head pressure.

For the wells having more uncertainity in the PI estimation, gauges are installed below the JP. Based on the gauge data, the model is revalidated and further optimization is done to obtain better JP efficiency while maintaining the desired liquid rates.

Overall, continuous surveillance, modeling, and regular optimization have helped to increase the JP efficiency while maintaining the production.

Jet Pump Operating Challenges

Scaling in JP: Thumbli aquifer water along with produced water is used as power fluid for JP and water injection. With the increase in WC, scaling has been observed in some of the JPs. The dominant scale type in the Mangala wells is:

- Barite scale: Thumbli injection water is rich in sulfate whereas Mangala formation water contains Barium, and mixing of these two incompatible water under the available pressure and temperature conditions causes barite scale. This barite scale has been observed in various wells during production logging (PLT's) as an increased gamma ray peak.

At the JP throat, produced water and PF water mixes and provides an ideal place for barite scaling. The deposition of scale causes PF rate decline and hence loss in liquid production. Additionally, the loss of JP performance due to scale required regular well interventions to change the JP. Post retrieval of JP, the scale sample from the wells has been analyzed by solubility tests and X-ray diffraction (XRD) and both methods indicated that the scale predominantely contained barite.

Fig.7 shows the scaling tendency in well A. The well is equipped with a permanent downhole gauge (PDG) located about 10 meters below the JP depth. As the water cut increased in the well, the liquid rate declined and a JP was installed to restore the liquid production rate. Within 3-4 days of operating the JP, the intake pressure started increasing and hence liquid production declined. Subsequent to this, the JP was retrieved for investigation and internals were found to be scaled. Fig. 8 shows the scale deposition observed in the JP retrieved from the well. The JP was changed out and again scale formation was observed within few days. The well's production rate was varied rapidly (rocked) in an effort to dislodge the scales, and the intake pressure decreased; however the intake pressure again started increasing slowly (Fig. 9). To tackle the scaling issue, downhole scale inhibitor was started on a pilot basis in this well. This was achieved using 3/8" capillary line terminated below JP depth at a chemical injection mandrel already provided in the completion. No scaling tendency was observed post

downhole injection and the well produced at a stable intake pressure.

Similar scaling tendency was observed in a few other wells, and downhole scale inhibition was done on need basis. However, with the increase in field WC, severe scaling was observed in many wells (Fig.10), and this resulted in frequent changeout of the JP and also loss in production as surface facility was not available for pumping downhole scale inhibitor in multiple wells located at same wellpad.

From the beginning of jet pumping in the field scale inhibitor dosing was being done at 5 ppm in the PF network. Due to inability to pump scale inhibitor in multiple wells as stated above, it was decided to increase the scale inhibitor dosing from 5 to 15 ppm in the PF network. Following this, the scaling tendency was arrested to a large extent. Fig. 11 shows fairly stable PF rate post increase in scale inhibitor dosing in the same well A.

In another well, scaling was mainly observed at the pump suction, upstream of the JP throat. (Fig 12). Although this well did not show any decline in PF rate, the liquid rate declined multi-fold. Upon investigation, it was observed that as this well was close to the oil water contact (OWC), it was producing both formation and Thumbli injection water which possibly caused scaling at the sand face and completion upstream of the JP.

Insert Cage Damage. In some of the wells, decline was observed in the PF rate without any change in surface pumping pressure. This was a normally a sudden phenomena compared to scaling case where the decline was gradual. Upon investigation, it was observed that insert cage which houses the check valve was getting damaged. Later on metallurgy was changed and the cage rib size was increased which prevented similar failure in subsequent installations (Chavan et al.).

Metering: Accuracy of multiphase metering has always been a challenge; the inclusion of PF along with produced fluid in the meter brings an additional complexity. To calculate the WC in such wells, PF rate measured from the single phase meter installed at the PF inlet has to be subtracted from the total liquid measured by the MPFM. Although single phase meters have higher accuracy, but occasionally they can get out of range and this can lead to spurious welltest measurement. It is essential to crosscheck the PF and well liquid rate from wellhead basic sediment and water (BS&W) sample as well as well model.

Standing Valve: During initial trials, JPs were installed after setting a standing valve in the nipple profile below jet pump. This practice was followed to avoid any accidental bull heading of power fluid in the well which may occur due to accidental shut-in of the well. In one of the well, due to production of sand, the retrieval of standing valve became difficult. Also, the additional restriction (smaller internal diameter) in standing valve caused extra pressure drop in case of high liquid producing well. Once the operational confidence in JP was gained and additional procdures were implemented to avoid accidental bullheading, it was decided not to use standing valve inthe subsequent wells.

Packer Failure: Approximately half of the Mangala wells were completed with a retrievable packer. Initial study suggested that the packer will be able to withstand various loads expected during jet pumping. However, after the onset of jet pumping, packer failure has been reported in more than 10 wells. Preliminary investigations have attributed these failures to the cyclical loads caused by fluctuations in the power fluid pressure, including surface power fluid pump trips. In all wells where such failures have been reported, semi-permanent/permanent packers have been installed. Also to avoid failure in the existing wells competed with retrievable packer; stringent procedure of gradual ramp up/down of PF has been implemented. This has helped to reduce the cases of packer failure in such wells. By continuous monitoring of wells using DOF, large volume bullheading into the formation in case of packer failure has been avoided.

Optimized JP size installation: Initially, number of wells flowing on JP was small and JP vendor technician was called out occasionally in case of new JP size requirement for installation/changeout. Based on prediction of JP size required in the forthcoming wells, some extra JP combinations were always available in field for installation. However, with the increase in frequency of JP changeout and installation activities, it was observed that sometimes inefficient JP's were being installed because of unavailability of the suitable size on immediate basis. These inefficient JP installations not only reduced the liquid production but also caused extra water handling in the plant. With more than 90 wells on JP in the field and increased requirement of JP change-out, a field based team of inhouse JP technicians was created for quickly redressing JPs. This has helped in installing the most efficient and optimal JP in the wells without any delay.

JP stalling:JP stalling is a condition in which there is no influx from reservoir and only PF is circulated through JP and tubing. This condition has been achieved by increasing THP and also loweing the PF rate for the instlled JP in Mangala well. The value for THP and PF pressure/rate to achieve pump stalling condition can be estimated from the industry standar software. This will further help in optimizing completion design in terms of flow assurance.

JP Modeling and Challenges

Initial JP modeling was done using various industry standard modeling software packages. Although these software were able to approximately model the required result, each had their own limitations. The main issues observed were for the PF rate determination, pump stalling prediction, limited vertical lift performance correlations, and unavailability of actual loss coeffiecients from the manufacturer.

Given the limitation of available JP design software, it was necessary to develop an algorithm based on available literatures.

JP Design Algorithm Development and Experimental Observations

This section of the paper is an attempt to provide field data support to theoretical curves and observations published in Grupping et al's paper "Fundamentals of Oil Well Jet Pumping, SPE Production Engineering, February 1988". Actual field data has been plotted on the curves to support their validity. This paper will follow the same nomenclature and symbol conventions as used in the Grupping's paper.

Fig. 13 shows a simplified drawing of the components of a JP. Power fluid with pressure P_n and at rate q_n is pumped through a nozzle with flow area A_n. This produces a high-velocity jet with pressure P_e at the throat entrance. Well fluid with pressure P_p and at rate q_f is accelerated into the suction area, A_e, and mixes in the throat with the power fluid to form a homogeneous mixture that leaves the throat with pressure P_t. In the diffuser section of the JP, the mixture velocity reduces and pressure builds up to the pump discharge pressure, P_d, which is sufficiently high to lift the mixture to surface.

The dimensionless nozzle-to-throat-area ratio of a jet pump is defined as $A_n/A_t=F_{AD}$ and consequently $A_e/A_t=1-F_{AD}$ and $A_e/A_n = (1-F_{AD})/F_{AD}$.

In the analysis of jet pumping, two dimensionless parameters are defined: the dimensionless mass flow ratio,

$$Fwd = \frac{q_f * \rho_f}{q_n * \rho_{pf}} \quad \ldots\ldots\ldots\ldots\ldots\ldots\ldots\ldots\ldots\ldots\ldots\ldots\ldots\ldots (1)$$

And the dimensionless pressure recovery ratio,

$$F_{pD} = \frac{Pd - Pp}{Pn - Pd} \quad \ldots\ldots\ldots\ldots\ldots\ldots\ldots\ldots\ldots\ldots\ldots\ldots\ldots\ldots (2)$$

Fig. 14 shows, the pressure trend of power fluid and produced fluid in a jet pump.

On solving the pressure losses equations across nozzle, diffuser, and suction and momentum conservation equation in throat, dimensionless pressure recovery ratio can be expressed as:

$$F_{pD} = \frac{2F_{AD} + [1-(2F_{AD})]\left[\frac{F_{wD}{}^2 F_{AD}{}^2}{(1-F_{AD})^2}\right]\left(\frac{\rho_{pf}}{\rho_f}\right) - (1+K_{td})(F_{wD}+1)^2 F_{AD}{}^2 \left(\frac{\rho_{pf}}{\rho_M}\right)}{1+K_n-n} \quad \ldots\ldots\ldots\ldots\ldots\ldots (3)$$

And efficiency equation can be expressed as:

$$E = F_{wD}F_{pD}\left(\frac{\rho_{pf}}{\rho_f}\right) \quad \ldots\ldots\ldots\ldots\ldots\ldots\ldots\ldots\ldots (4)$$

F_{wd} is expressed as:

$$Fwd = \left(\frac{q_f}{q_n}\right)\left(\frac{\rho_f}{\rho_{pf}}\right) \quad \ldots\ldots\ldots\ldots\ldots\ldots\ldots\ldots\ldots\ldots\ldots\ldots\ldots\ldots (5)$$

And

$$\rho_M = \frac{q_f\rho_f + q_n\rho_{pf}}{q_f + q_n} \quad \ldots\ldots\ldots\ldots\ldots\ldots\ldots\ldots\ldots\ldots\ldots\ldots\ldots\ldots (6)$$

It follows that,

$$\frac{\rho_{pf}}{\rho_M} = \frac{(F_{wD})\left(\frac{\rho_{pf}}{\rho_f}\right)+1}{F_{wD}+1} \quad \ldots\ldots\ldots\ldots\ldots\ldots\ldots\ldots\ldots\ldots\ldots\ldots\ldots\ldots\ldots (7)$$

Following this, Grupping's paper has mentioned that higher efficiencies can be obtained by pumping a low-density

production with a high-density power fluid than vice versa.

Next observation that Grupping et al has mentioned in their paper[1] is based on the following equation:

$$\frac{P_e}{P_p} = 1 - \left[\frac{\left(F_{wD}{}^2\right)\left(F_{AD}{}^2\right)}{(1-F_{AD})^2(1+K_n)}\right]\left[\frac{P_n}{P_p} - 1\right]\left(\frac{\rho_{pf}}{\rho_f}\right) \ldots\ldots\ldots\ldots\ldots (8)$$

With the help of Eqs. 3 & 8, a plot of pump efficiency vs. P_e/P_p for various values of F_{AD} and P_n/P_p was plotted (Fig. 16). This was obtained by solving Eqs. 3&8 for a number of F_{wD} values and calculating the corresponding efficiency values. Based on that plot, Grupping et al has made the following observation:

"*For all values of F_{AD}, the pumping process will take place most efficiently for P_e/P_p values in the range of 0.3 to 0.7.*"

This paper will make an attempt to validate the following two observations with the help of actual field data/ examples:

1. Efficiency increases with increase in the ratio of $\frac{\rho_{pf}}{\rho_M}$, i.e. higher efficiencies can be obtained by pumping low-density produced fluid with a high-density power fluid.
2. Maximum efficiency will be obtained when the ratio of throat-entrance pressure to pump intake pressure is in the range of 0.3 to 0.7.

Field dataset:

13C (F_{AD} = 0.234) jet pump was installed in a well (well B) with downhole gauges to continuously monitor the pump suction pressure. Following steps were followed to model the Jet pump and match the measured suction pressure:

1. For the known PI and reservoir pressure of the well, Inflow Performance Relation (IPR) at reservoir depth is calculated. By using a proper Vertical Lift Performance (VLP) correlation and with the help of nodal analysis software, IPR at pump suction depth is calculated.

2. For each suction pressure and reservoir liquid production at the pump suction depth IPR, throat entry pressure is calculated using the folllowing equation

$$P_p - P_e = \frac{1}{2}\left(\rho_f {v_f}^2\right) \ldots\ldots\ldots\ldots\ldots\ldots\ldots\ldots\ldots\ldots\ldots\ldots\ldots\ldots (9)$$

(ρ_f, *fluid density at P_p is calculated using PVT lookup table for the reservoir fluid*)

3. For the given surface injection pressure, nozzle pressure at pump depth (P_n) was calculated using the nodal analysis software. With the known P_n and P_e, power fluid rate v_{fpf} was calculated using the following nozzle equation:

$$P_n - P_e = (1 + K_n)\left[\frac{1}{2}\left(\rho_{pf} {v_n}^2\right)\right] \ldots\ldots\ldots\ldots\ldots\ldots\ldots\ldots\ldots\ldots (10)$$

(*Value of K_n is used as* 0.03)

4. With the rate and density of both power fluid and reservoir fluid known and expressing the areas in terms of $F_{AD} = {A_n}/{A_t}$, throat exit pressure is calculated using following equation:

$$P_t - P_e = \left(F_{AD}\rho_{pf}{v_n}^2\right) + (1 - F_{AD})\left(\rho_f {v_f}^2\right) - \left[1 + {1}/{2}\, K_t\right]\left(\rho_m {v_m}^2\right) \ldots\ldots\ldots\ldots\ldots\ldots\ldots\ldots (11)$$

(ρ_m, *mixture density is calculated as* $\rho_m = \frac{\rho_f q_f + \rho_{pf} q_{pf}}{q_f + q_{pf}}$ *and value of K_t used is* 0.1)

5. With throat exit pressure known, discharge pressure curve was calculated corresponding to each point on suction IPR curve using following equation:

$$P_d - P_t = (1 - K_d)\left[{1}/{2}\,\left(\rho_M {v_M}^2\right)\right] \ldots\ldots\ldots\ldots\ldots\ldots\ldots (12)$$

(*Value of K_d is used as* 0.1)

6. Now for the given well THP and total fluid (reservoir + power fluid) produced from the well, VLP is used to calculate the pump discharge pressure. The intersection of the two curves (discharge pressure using VLP and using Grupping et al equation) provides the solution point for the well.

By using the equations for all the pressures (nozzle, throat, suction and discharge) and expressing the equations in terms of F_{AD}, F_{wD} and using a combined throat diffuser loss co-efficient, Eq. 3 is obtained.

The above steps provided a reasonable match for the measured data of well B. Subsequently, additional five cases from 3 different wells producing with different WC and different GOR were matched. Description of cases and results are mentioned in Table 3.

Now, these data points were plotted on the curves mentioned in the Grupping et al paper to validate the following statements mentioned earlier.

1. **Efficiency increases with increase in the ratio of $\frac{\rho_{pf}}{\rho_M}$**

a. Plotting the efficiency curve for all the six cases, it can be observed that maximum efficiency point is following the trend of increase in density ratio (Table-3) & Fig.15. However, in case-1 even though the density ratio is highest among all the cases, efficiency is lower than case-4 but it can be clearly seen that the pump is not operating at its highest efficiency but in all other cases operating point is close to the maximum efficiency point on the curve.

2. **Maximum efficiency will be obtained when the ratio of throat-entrance pressure to pump intake pressure (P_e/P_p) is in the range of 0.3 to 0.7**

a. Grupping et al have mentioned that in the above plot, jet pumping process will be most efficient for P_e/P_p value in the range of 0.3 to 0.7 for all values of $F_{AD.}$ However, concern was raised by Griffin over this observation which states that:
"*The conclusion that maximum efficiencies will be obtained when the ratio of throat-entrance pressure to pump intake pressure is in the range of 0.3 to 0.7 is in error and is not borne out by experience or experiment. Grupping et al reached this conclusion by Fig. 16, which is a plot of efficiency vs. the aforementioned ratio for constant values of nozzle pressure/pump-intake pressure. But for a given problem for specified production rate and pump-intake pressure, the nozzle pressure will vary as throat-intake pressure varies because varying throat intake pressure means varying nozzle and throat size*."

This was acknowledged by Grupping and he clearly stated in his reply that changing P_n/P_p ratio will change Pe values but it doesn't invalidate the plot and there will be different curves for different P_n/P_p ratios. Also these curves were plotted for constant $\frac{\rho_{pf}}{\rho_f}$.
But for a multiphase pumping system, change in P_n/P_p will not only vary P_e/P_p but also $\frac{\rho_{pf}}{\rho_f}$ where ρ_f will vary with change in suction pressure P_p. Hence in plotting the curves this variation will have to be taken into account as per *Eq. 8*. Based on the above discussions, for the six cases six different curves were made and field data points were plotted on the curves. All the cases were for F_{AD}= 0.234. As seen in the *Fig-16* and *Table-3*, all the cases were lying around P_e/P_p values of 0.7 with one value (Case-5) of 0.85.

b. The other observation is that with increase in P_n/P_p ratio there is an increase in $\frac{\rho_{pf}}{\rho_f}$ and $\frac{\rho_{pf}}{\rho_M}$ values and maximum efficiency values increases with maximum efficiency point moving towards the lower P_e/P_p values. In our cases, P_n is fairly constant as pumps were operating at the maximum surface injection pressure, so decrease in P_e/P_p ratio with increase in P_n/P_p implies that there is decrease in suction pressure (P_p) as well as throat entrance pressure (P_e).

Based on the above observations, it can be concluded that:

1. Lowering of P_e/P_p values will have higher efficiencies at all values of F_{WD} for a given fluid system as the controlling factor for the plot (Fig. 16) is the density ratio $\frac{\rho_{pf}}{\rho_f}$ or $\frac{\rho_{pf}}{\rho_M}$. P_e/P_p curves for lower P_n/P_p values (lower density ratio, $\frac{\rho_{pf}}{\rho_f}$) will have their maximum efficiency for P_e/P_p values in the range of 0.7 and P_e/P_p curves for higher P_n/P_p (higher density ratio, $\frac{\rho_{pf}}{\rho_f}$) values will have their maximum efficiency for P_e/P_p values in the range of 0.3 (as per the plots). Beyond these ranges, the efficiency will be following a declining trend for both the cases.

2. Another observation can be made from a similar plot (Fig. 17) which shows the plot of P_e/P_p and efficiency vs F_{wD} for Case-4 & Case-5. It can be seen that decrease in the P_e/P_p ratio (increase in $\frac{\rho_{pf}}{\rho_f}$ ratio) increases the efficiency for a multiphase flow system but the cut-off F_{wD} value is reduced. If there has been no change in density ratio, lowering of P_e/P_p value will follow a single curve and F_{wD} will increase for every step decrease in P_e/P_p ratio. But, this is not the case for a multiphase system containing free gas in the system. Lowering of P_e/P_p value in effect will increase the free gas in the system and hence will increase the density ratio which in effect will narrow down F_{wD} value for the system.

However, the plot (*Fig. 16*) based on the theoretical equations extend up to values of zero Pe/Pp which in effect means creating a vaccum at throat inlet which is not physically possible. Also, the lower limit value of Pe/Pp ratio of 0.3 may not be applicable for a multiphase fluid system with a high GOR. This ratio could be higher and needs to be established from experiment and field measurements. Grupping et al has also mentioned in their paper that velocity at the throat entrance can become so high that they exceed this critical velocity of sound. When that happens, the suction flow rate does not respond any more to the further reduction of the throat suction pressure, Pe. This critical flow will be more severe with free gas present in the system and hence as per Grupping et al, Pe/Pp values higher than 0.5 should be aimed for. But then again, this value as mentioned earlier needs to be established for the given fluid system.

Similar phenomena have been observed in some of the Mangala JP Wells which is under further investigation.

Critical vs subcritical flow:

Critical flow is the rate at which fluid velocity is equal or above the sonic velocity in the medium. This phenomenon is very well understood and explained for flow across chokes in both oil and gas wells. If the flow is critical then any disturbance downstream of choke doesn't affect upstream pressure.

Air sonic velocity is typically ~340 m/sec and water sonic velocity is ~ 1480 m/sec at 20^0C. It is interesting to note that the gas and water mixture sonic velocity is much lower than even the gas/air sonic velocity (Fig 19). Thus critical flow condition can easily occur in case of JP used for pumping multiphase fluid.

Future Modeling Scope:

The authors believe that the current commercially available software have certain limitation in terms of designing, optimizing and predicting capability of JP. This has been mainly due to the fact that still there is a lot of confidentiality in terms of published loss coefficients from manufacturers and historically JP has not been as popular compared to other lift mechanisms like ESP, gas lift, SRP etc. Moreover most of the work on hydraulic lifts/JP has been done for single phase and complexities arise with the introduction of multiphase into the system. More collaboration between the operator and the manufacturer and the software development team may help in developing a more robust model in future.

The authors are currently working with external consultants to develop algorithms for jet pump modeling in multiphase flow to capture the critical flow behavior observed in Mangala wells. A separate paper shall be published in due course of time with the field data based on the modified algorithm capturing critical flow behavior.

Conclusions

Jet pumping has been succesfully implemented in Mangala field. With the handling of a significant number of wells on JP, there have been many learning in terms of operations and surveillance. It has been observed that the power fluid rate is mostly dependent on the nozzle size, jet pump depth and the power fluid pressure for a given completion. However, it is not affected by the throat size and THP for a given nozzle size. A detailed workflow has been developed incorporating the variance in power fluid rates and other wellhead parameters for monitoring and troubleshooting of the large number of JPs in the field. In the existing jet pump literature available in the user domain, there is not much discussion on the operational issues. The extensive use of jet pump in Mangala field has helped the operator to understand the issues such as scaling, packer failure, jet pump mechanical failure etc in detail and and develop in-house experise to deal with the issues which are covered in detail in the paper.

As per our experience, the software available in the market are limited in their approach to properly model the jet pump performance in multi phase flow. With the help of available literature, combined with the field observations a customized inhouse modeling tool has been developed, this has significantly helped in current optimization efforts. Field examples have helped in validating the two observations documented in the literature:

1. Efficiency increases with increase in the ratio of $\frac{\rho_{pf}}{\rho_M}$, i.e. higher efficiencies can be obtained by pumping low-density produced fluid with a high-density power fluid.
2. Maximum efficiency will be obtained when the ratio of throat-entrance pressure to pump intake pressure (Pe/Pp) is in the range of 0.3 to 0.7.

Also, it has been concluded that for a multiphase Jet pumping system, Pe/Pp values plays an important role in determining flow ratio cut-offs as well as cavitation. As per literature, this ratio should be aimed for higher than 0.5 but this value needs to be established for field specific fluid systems and conditions.

With future work, including the incorporation of critical flow behavior, the modeling tool is expected to open new scope for effective jet pump sizing and optimization in case of multiphase reservoir fluid.

Acknowledgement
The authors would like to thank Cairn India Limited (CIL) and its Joint Venture partner Oil and Natural Gas Corporation Limited (ONGC) for their permission to publish this paper.We would like to thank Mr. Piyush Kumar and Mr. Sanjeev Kumar from CIL for their significant contributions at various stages of this project.

Nomenclature

A_e	Flow area of throat entrance, At – An
A_n	Flow area of nozzle,
At	Flow area of throat
BOPD	Barrels of Oil per Day
BLPD	Barrels of Liquid per Day
BS&W	Basic Sediment and Water
DOF	Digital Oil Field
E	Pump efficiency
ESP	Electrical Submersible Pump
F_{AD}	Dimensionless nozzle-to-throat-area ratio
F_{pD}	Dimensionless pressure-recovery ratio
F_{wD}	Dimensionless mass flow ratio
FT	Flow transmitter
GOR	Gas Oil Ratio
GR	Gamma Ray
ID	Internal Diameter
IPR	Reservoir Inflow Performance
JP	Jet Pump
K_d	Diffuser-loss coefficient
K_n	Nozzle-loss coefficient
K_{sl}	Suction-loss coefficient
Kt	Throat-loss coefficient
K_{td}	Throat/diffuser-loss coefficient
L	Distance from nozzle tip to throat entrance
m/sec	Meter/second
MPFM	Multi Phase Flow Meter
n	Value of numerator in eq. 3
OWC	Oil Water Contact
P_d	Pump discharge pressure
P_e	Throat entry pressure
P_n	Nozzle entrance pressure
P_p	Pump intake pressure
P_s	Pump suction pressure
P_t	Throat discharge pressure
PCP	Progressing Cavity Pump
PDG	Permanent Downhole Gauge
PF	Power Fluid
PI	Productiviry Index
PLT	Production Logging Tool
q_f	Flow rate of well fluids

q_m Flow rate of mixture of well fluids and power fluid
q_n Flow rate of power fluid through nozzle
ρ_f Density of well fluid
ρM Density of mixture of power fluid and well fluids in throat
ρ_{pf} Density of power fluid
SRP Sucker Rod Pump
SS Sub Surface
STOIIP Stock Tank Oil Initially in Place
TDS Total Suspended Solids
THP Tuving Head Pressure
TVD True Vertical Depth
VLP Vertical Lift Performance
WC Water Cut
WDT Wax Dissolution Temperature
WHP Well Head Pressure
WHT Well Head Temperature
XRD X-Ray Diffraction

References

1. Chavan, C., Jha, M., Singh, M.K., and Singh, R. (2012) Selection and Succesful Application of Jet Pumps in Mangala Oil Field: A Case Study. SPE 163116-MS. Presented at the SPE Artificial Lift Conference and Exihibition, Bahrain, 27-28 November
2. Research on Jet Pumps for Single and Multiphase Pumping of Crudes by J.C. Corteville et al-1987, SPE paper no. 16923
3. Petrie H.L., Wilson P.M. and Smart E.E. “Jet Pumping Oil Wells”, World Oil, p. 51 (Nov.1983)
4. Hydraulic Jet Pumps prove Ideally Suited for Remote Canadian Oil field, SPE paper no. 94263, J Anderson et al,2005
5. The technology of artificial lift methods, Kermit E. Brown etal.
6. Fundamentals of Oilwell Jet Pumping by A.W. Grupping, J.L.R. Coppes and J.G. Groot, SPE Production Engineering, February 1988
7. HIMR, D., HABAN, V., and Pochly, F., (2009) Sound Speed in the Fluid-Gas Mixture. 3rd IAHR International meeting of the Workshop on Cavitation and Dynamic Problems in Hydraulic Machinery and Systems,Brno, Czech Republic, 14-16 October

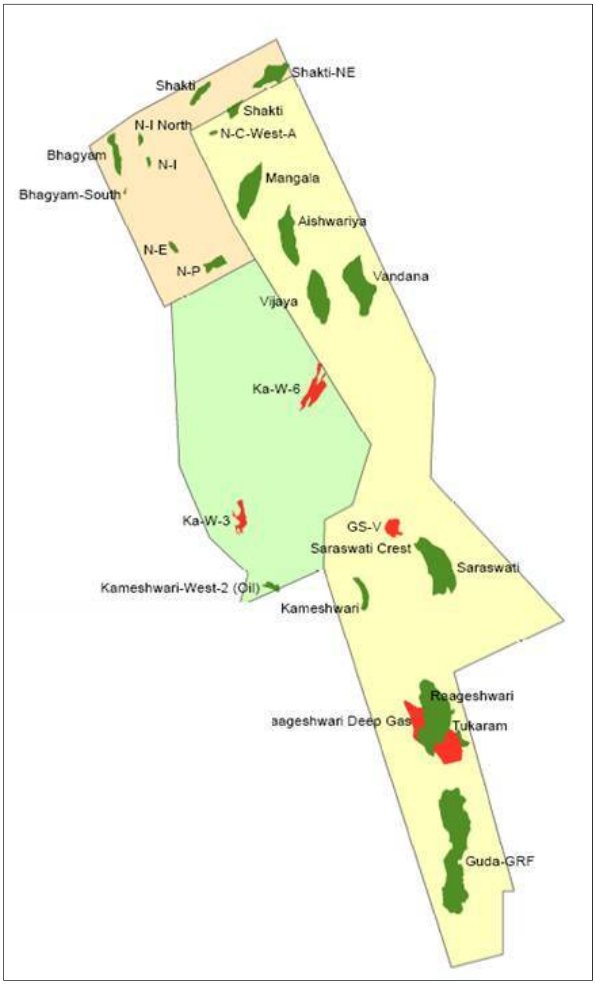

Fig.1: RJ-ON-90/1 Block

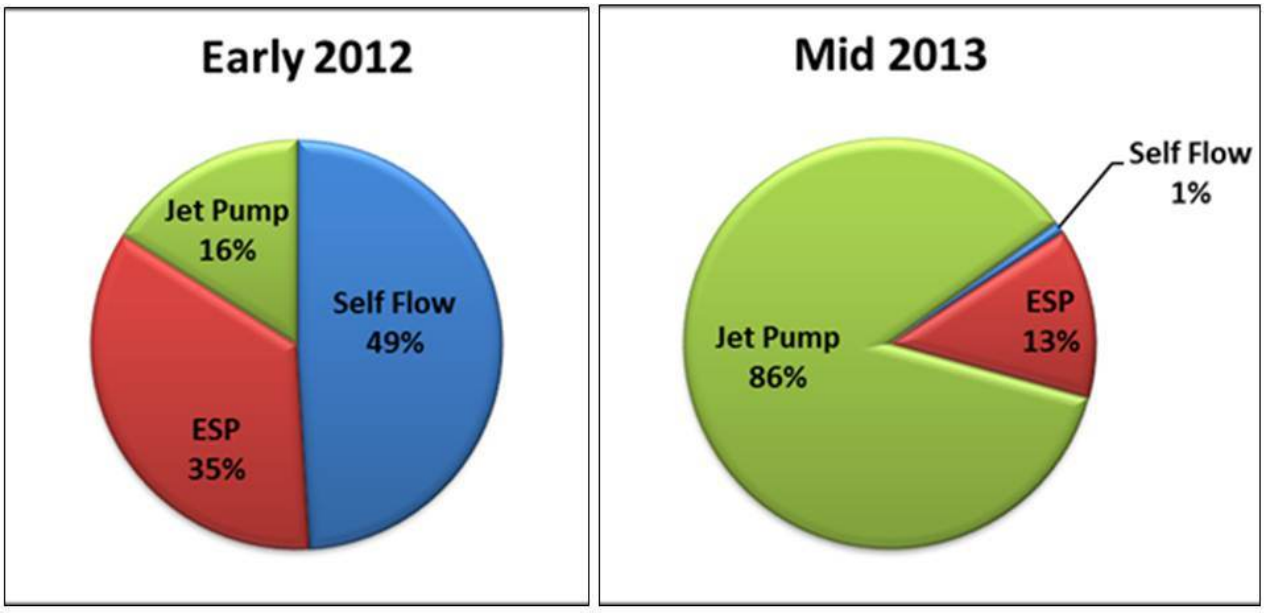

Fig. 2: Contribution from different lift mechanisms

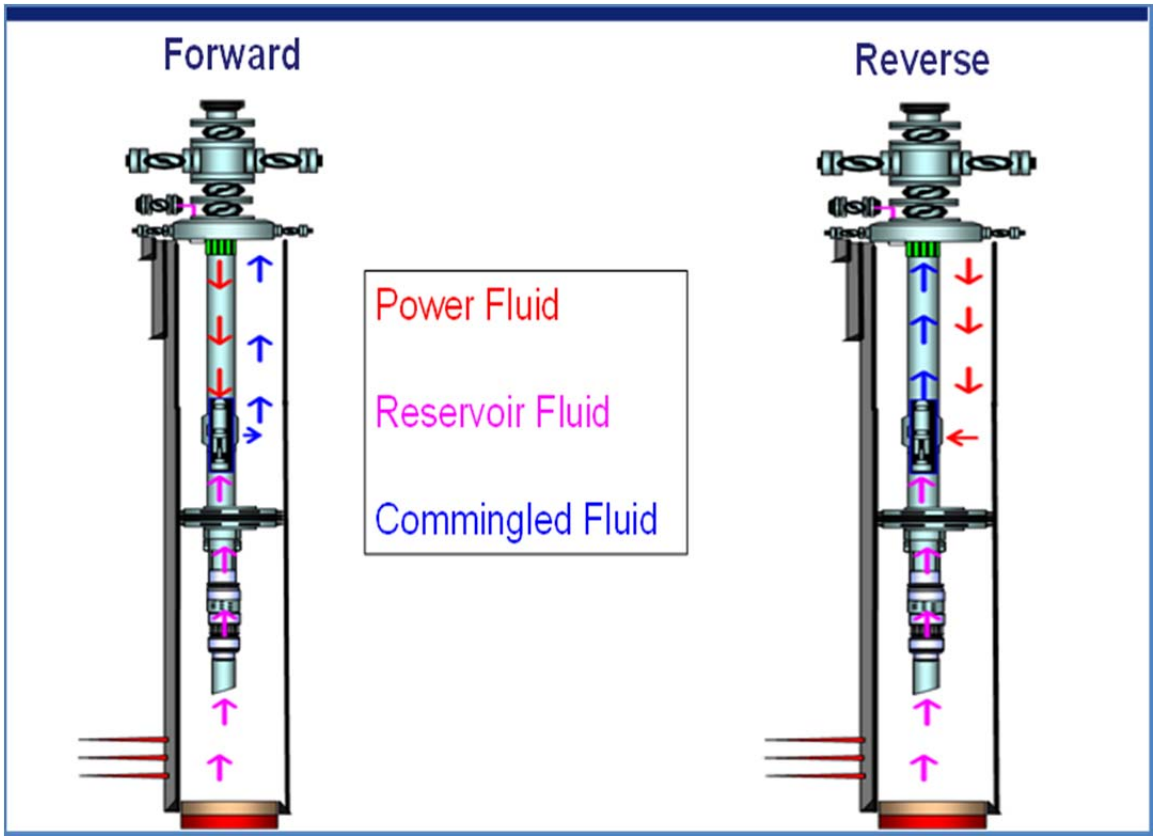

Fig. 3: Jet Pump Types – Forward and Reverse

Parameters	Unit	Range
Water Cut	%	25%
Gas Oil Ratio	Scf/stb	180-300
Oil Viscosity	Cp	18
Reservoir temperature	degC	65
Reservoir Pressure @ Datum 960m TVDSS	Psia	1620
WAT (Wax Appearance Temperature)	degC	59
WHP (Well Head Pressure)	Psi	170-250
Reservoir Liquid Rate	Bbl/day	200-8000
Pump setting depth	M	800-1000m
Typical Nozzle size	OilMaster	6-17
Typical Throat size	Oilmaster	C-E
Pump Intake Pressure	psi	700-1100
Power Fluid Pressure	Psi	2000-2300
Power Fluid Flow Rate	Bbl/day	600 (6B)- 6500 (17C)
Power Fluid to Produced Fluid Ratio	Fraction	0.5-1.1

Table 1: Typical Reservoir, Fluid and Jet Pump Parameters

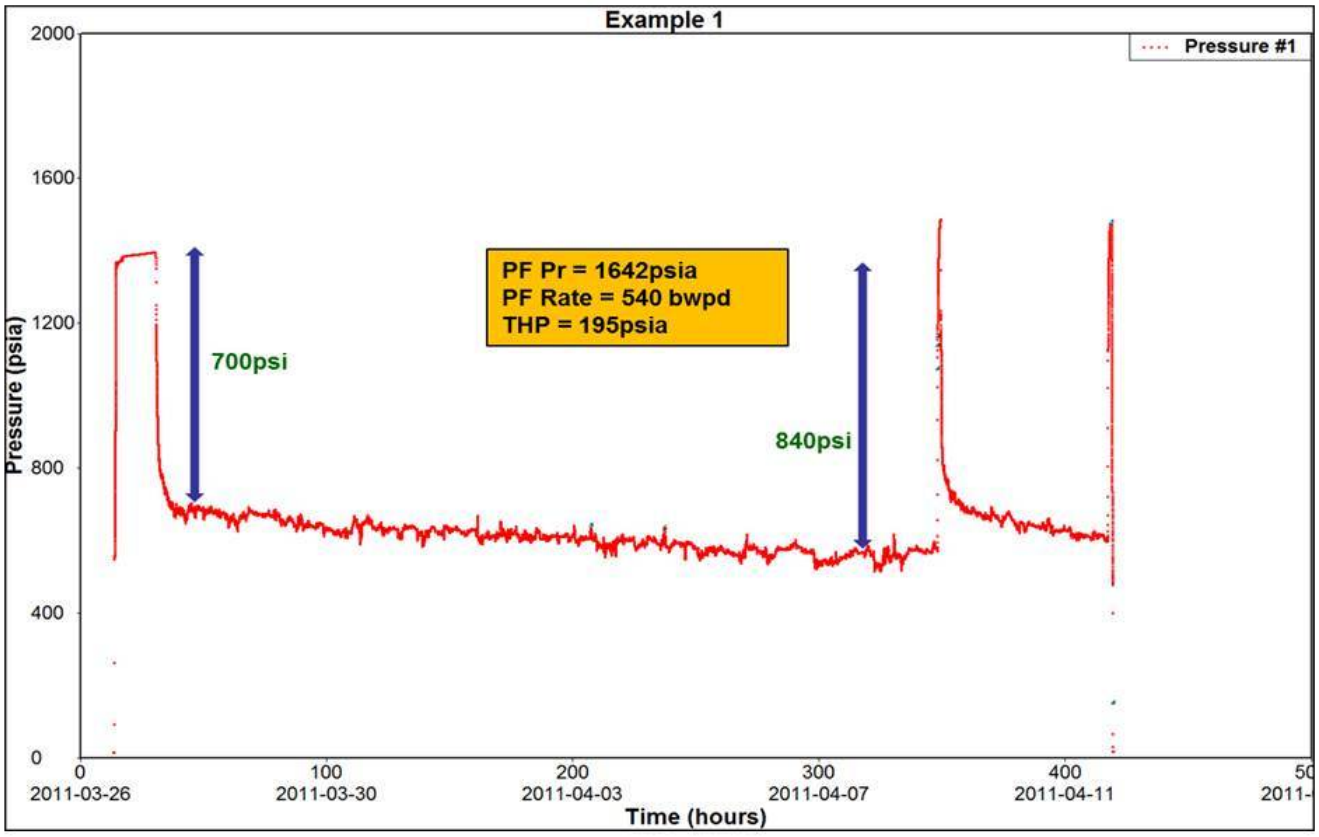

Fig. 4: JP Gauge Data from a Well with ~800 psi Drawdown (Size-7C)

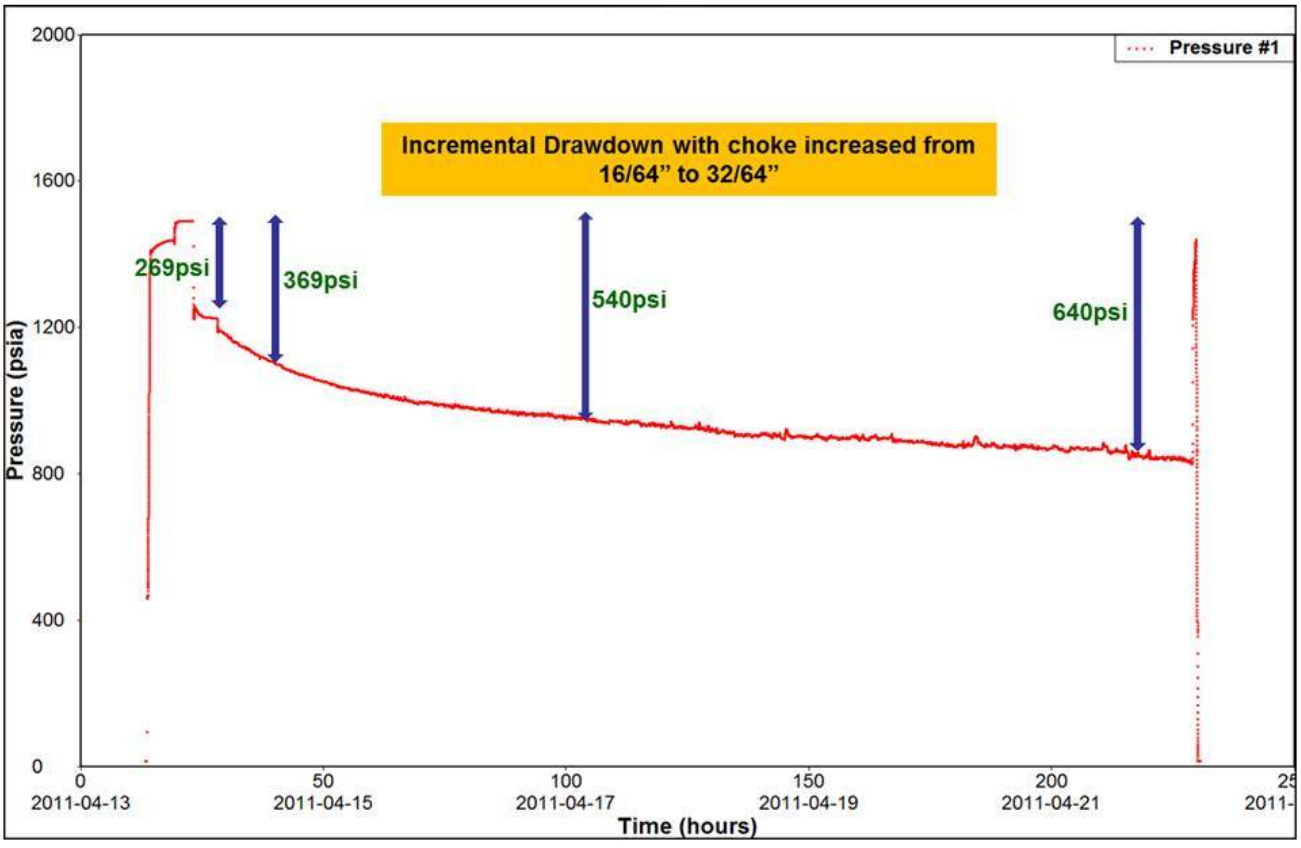

Fig. 5: JP Gauge Data from a Well Showing Incremental Drawdown

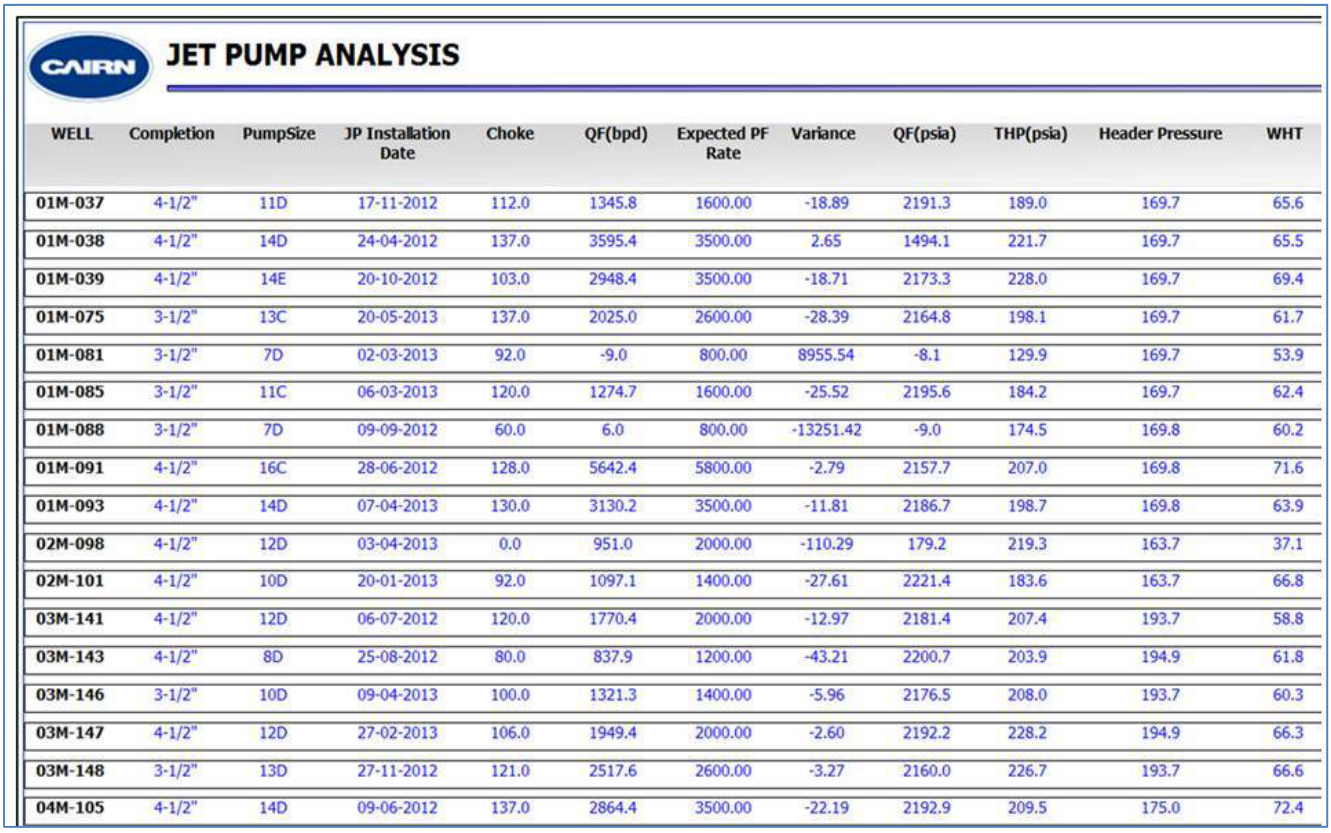

CAIRN

JET PUMP ANALYSIS

WELL	Completion	PumpSize	JP Installation Date	Choke	QF(bpd)	Expected PF Rate	Variance	QF(psia)	THP(psia)	Header Pressure	WHT
01M-037	4-1/2"	11D	17-11-2012	112.0	1345.8	1600.00	-18.89	2191.3	189.0	169.7	65.6
01M-038	4-1/2"	14D	24-04-2012	137.0	3595.4	3500.00	2.65	1494.1	221.7	169.7	65.5
01M-039	4-1/2"	14E	20-10-2012	103.0	2948.4	3500.00	-18.71	2173.3	228.0	169.7	69.4
01M-075	3-1/2"	13C	20-05-2013	137.0	2025.0	2600.00	-28.39	2164.8	198.1	169.7	61.7
01M-081	3-1/2"	7D	02-03-2013	92.0	-9.0	800.00	8955.54	-8.1	129.9	169.7	53.9
01M-085	3-1/2"	11C	06-03-2013	120.0	1274.7	1600.00	-25.52	2195.6	184.2	169.7	62.4
01M-088	3-1/2"	7D	09-09-2012	60.0	6.0	800.00	-13251.42	-9.0	174.5	169.8	60.2
01M-091	4-1/2"	16C	28-06-2012	128.0	5642.4	5800.00	-2.79	2157.7	207.0	169.8	71.6
01M-093	4-1/2"	14D	07-04-2013	130.0	3130.2	3500.00	-11.81	2186.7	198.7	169.8	63.9
02M-098	4-1/2"	12D	03-04-2013	0.0	951.0	2000.00	-110.29	179.2	219.3	163.7	37.1
02M-101	4-1/2"	10D	20-01-2013	92.0	1097.1	1400.00	-27.61	2221.4	183.6	163.7	66.8
03M-141	4-1/2"	12D	06-07-2012	120.0	1770.4	2000.00	-12.97	2181.4	207.4	193.7	58.8
03M-143	4-1/2"	8D	25-08-2012	80.0	837.9	1200.00	-43.21	2200.7	203.9	194.9	61.8
03M-146	3-1/2"	10D	09-04-2013	100.0	1321.3	1400.00	-5.96	2176.5	208.0	193.7	60.3
03M-147	4-1/2"	12D	27-02-2013	106.0	1949.4	2000.00	-2.60	2192.2	228.2	194.9	66.3
03M-148	3-1/2"	13D	27-11-2012	121.0	2517.6	2600.00	-3.27	2160.0	226.7	193.7	66.6
04M-105	4-1/2"	14D	09-06-2012	137.0	2864.4	3500.00	-22.19	2192.9	209.5	175.0	72.4

Fig. 6: Real Time JP Monitoring with DOF

THUMBLI (NR1) and Fatehgarh WATER ANALYSIS: OCTL			03/12/2005 Thumbli NR1	29/11/2004 Fatehgarh Ma-2
Name	Symbol	Units		
CATIONS				
Sodium	Na	(mg/l)	1395	2430
Calcium	Ca	(mg/l)	213	525
Magnesium	Mg	(mg/l)	113	87
Potassium	K	(mg/l)	18.3	190
Barium	Ba	(mg/l)	0.007	30
Iron	Fe	(mg/l)	0.03	1.3
Strontium	Sr	(mg/l)	4.55	2.8
ANIONS				
Chloride	Cl	(mg/l)	2343	4160
Sulfate	SO4	(mg/l)	445	8.5
Bicarbonate	HCO3	(mg/l)	209	867
GASES				
Carbon dioxide (free)/ Aq	CO2	(ppm)		2257
Oxygen (on site)	O2	(ppb)	80	
MISC				
Temperature		(degC)	~45	~70
pH			6.9 - 7.1	5.59
Total suspended solids	TSS	mg/l	2.5	
Total dissolved solids	TDS	mg/l	5500	9000

Table 2: Comparative Chemical Analysis of Thumbli Water and Mangala Formation Water

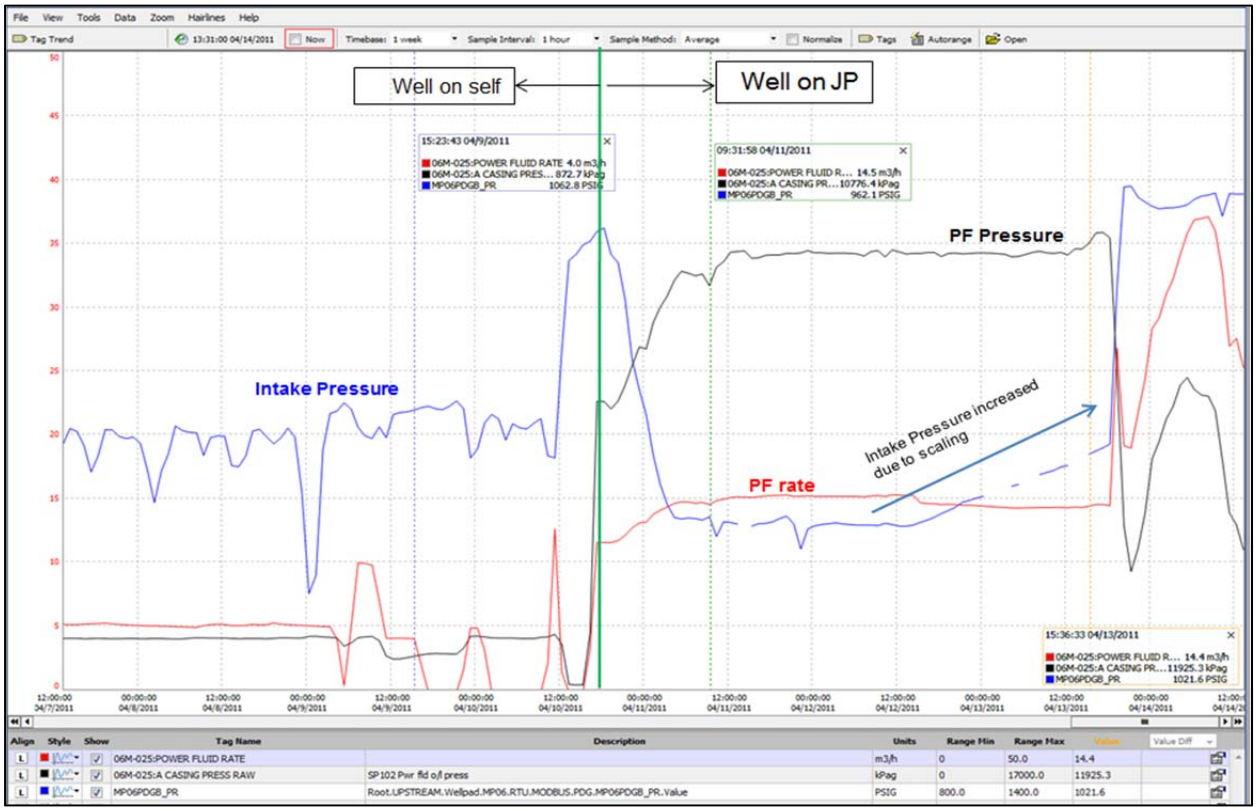

Fig. 7: Well A intake pressure rising due to scaling

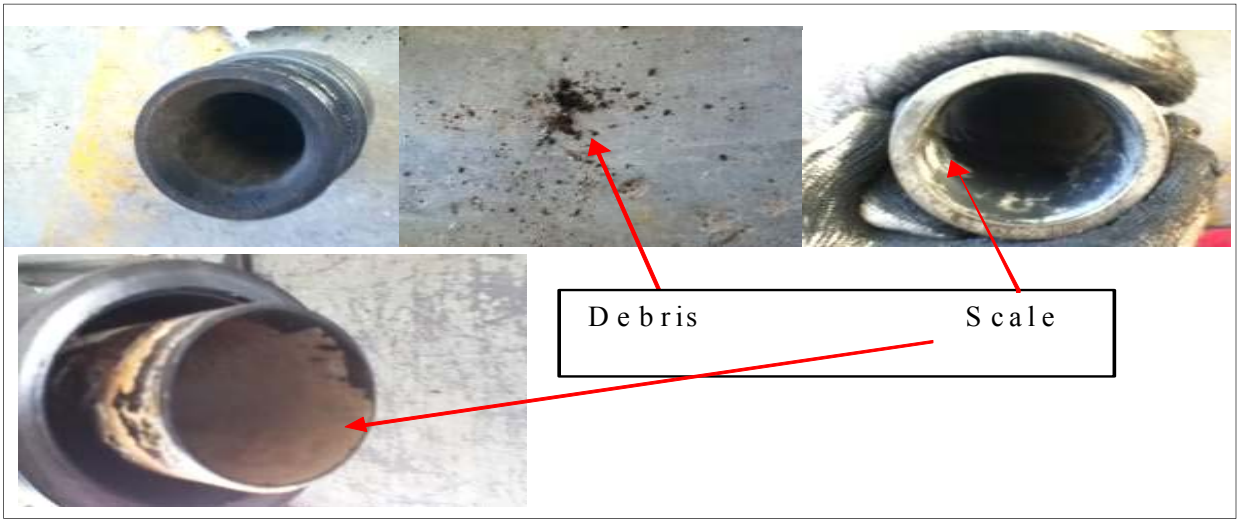

Fig. 8: Scale observed in Well A

Fig. 9: Well A-Rocking of well to dislodge scales

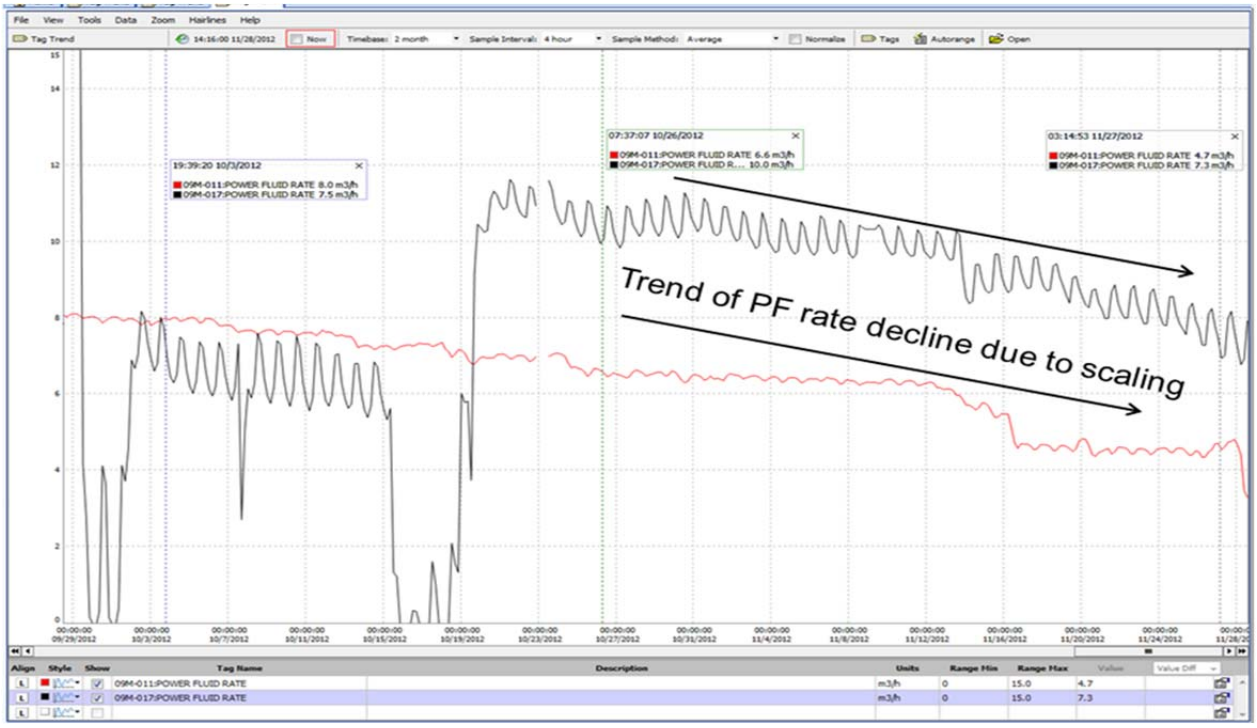

Fig. 10: PF rate declining in a well due to scaling

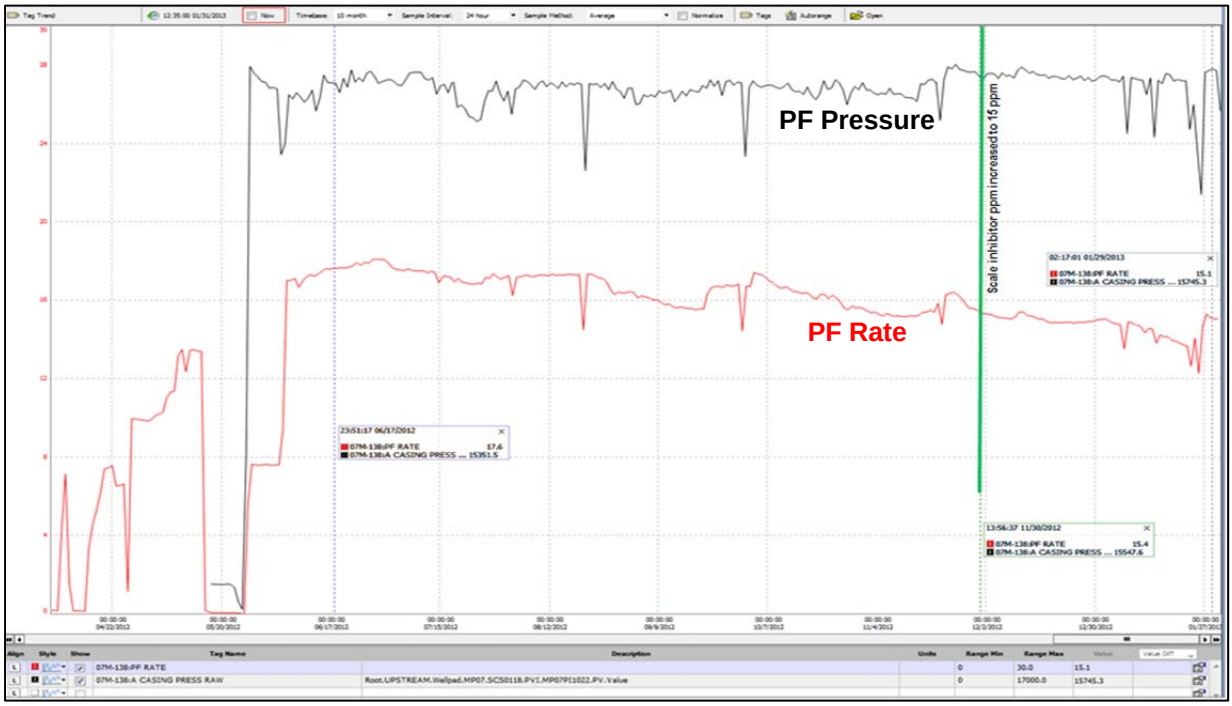

Fig. 11: Increase in Scale Inhibitor dosing controlled PF rate decline

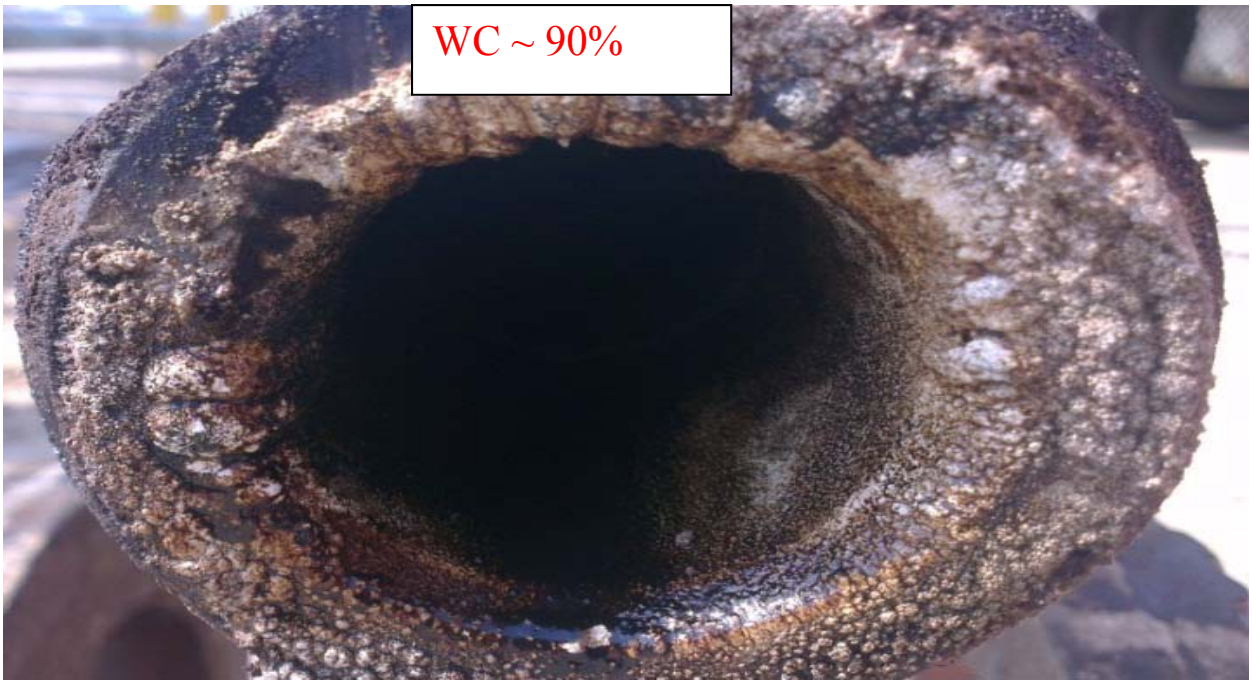

Fig. 12: Severe Scaling Observed in Jet Pump

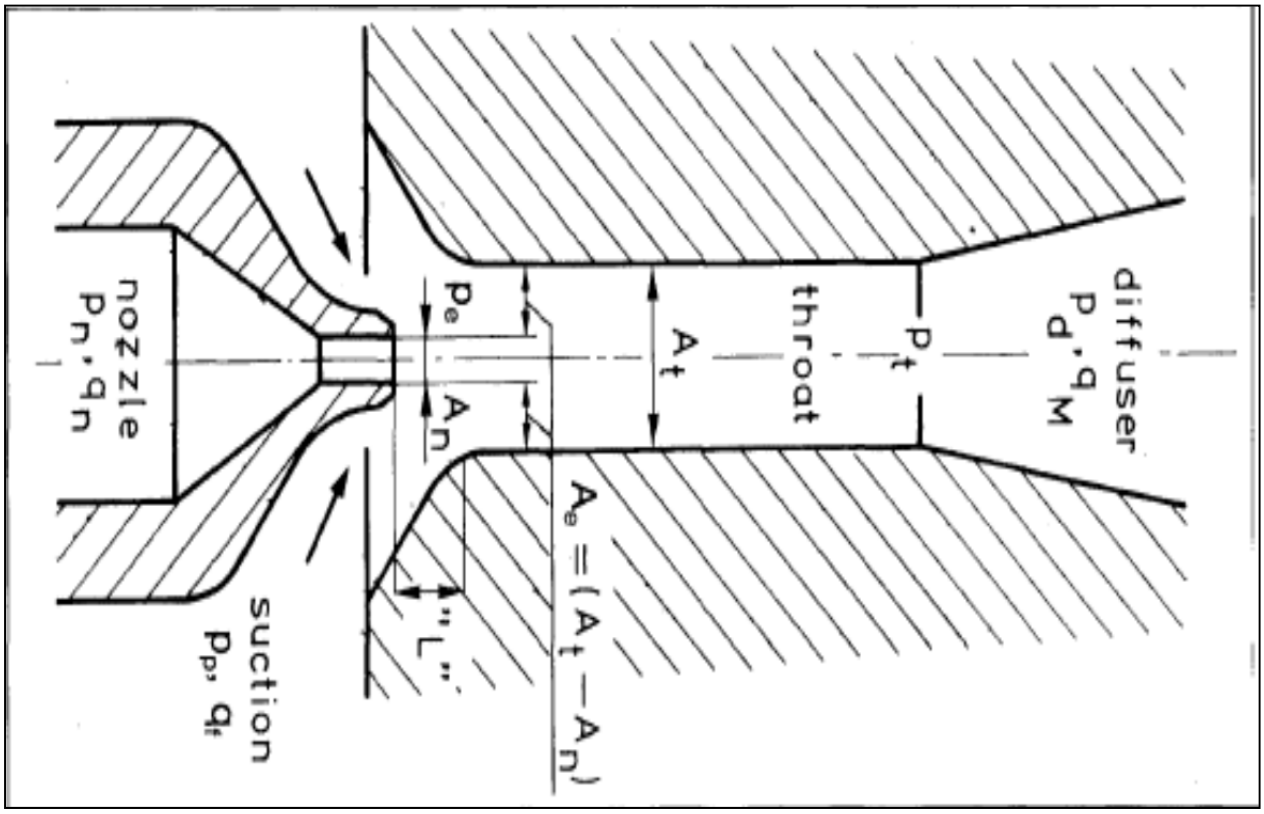

Fig. 13: Nomenclature for JP design calculations

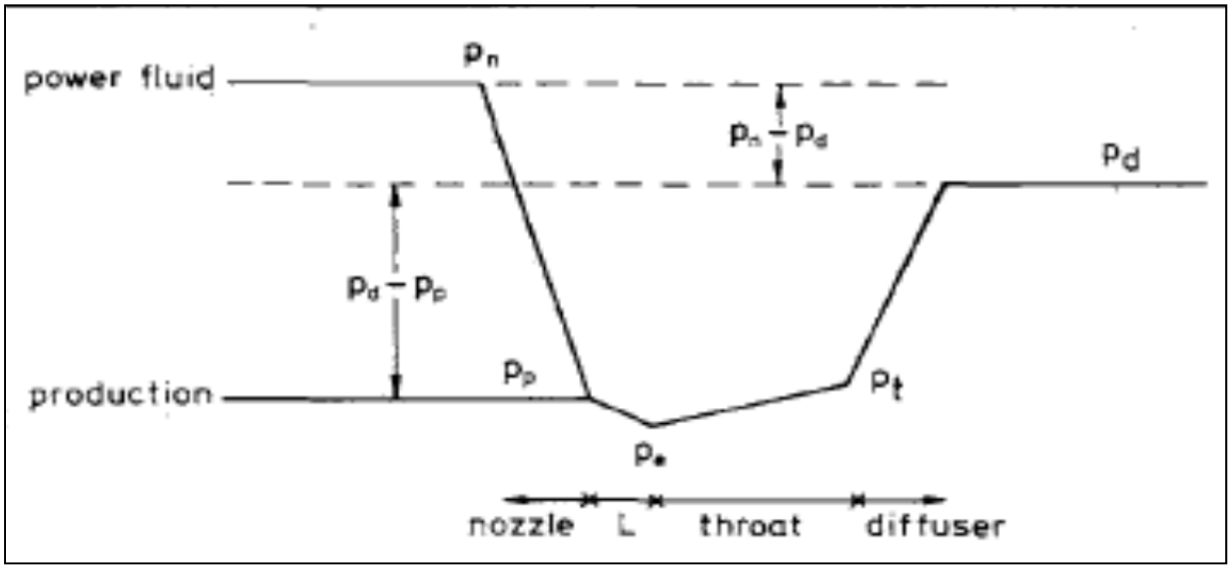

Fig. 14: Pressure trend of produced and power fluid in JP

	Well B		Well C		Well D	
	Case1	Case2	case3	case4	Case5	Case6
Res Liquid rate (blpd)	2015.0	1290.0	1270.0	3467.0	990.0	7700.0
PI (b/d/psi)	4.5	4.5	8.0	8.0	23.0	23.0
WC (%)	43.2	43.2	15.0	15.0	40.0	40.0
GOR (scf/stb)	190.4	190.4	200.0	200.0	245.0	245.0
Pe/Pp	0.723	0.686	0.729	0.700	0.851	0.739
Eff (fraction)	0.366	0.372	0.356	0.385	0.334	0.363
Pn/Pp	6.254	4.656	3.223	4.658	2.856	3.832
ppf/pf	1.486	1.309	1.167	1.423	1.055	1.226
ppf/pm	1.187	1.142	1.086	1.188	1.026	1.108
F_{pd}	0.393	0.334	0.284	0.339	0.345	0.325
F_{wd}	0.626	0.850	1.074	0.798	0.917	0.910
Nozzle No.	13	10	9	14	9	17
F_{AD}	C (0.234)	C (0.234)	C (0.234)	C (0.234)	C (0.234)	C (0.234)

Table 3: Results of JP modeling

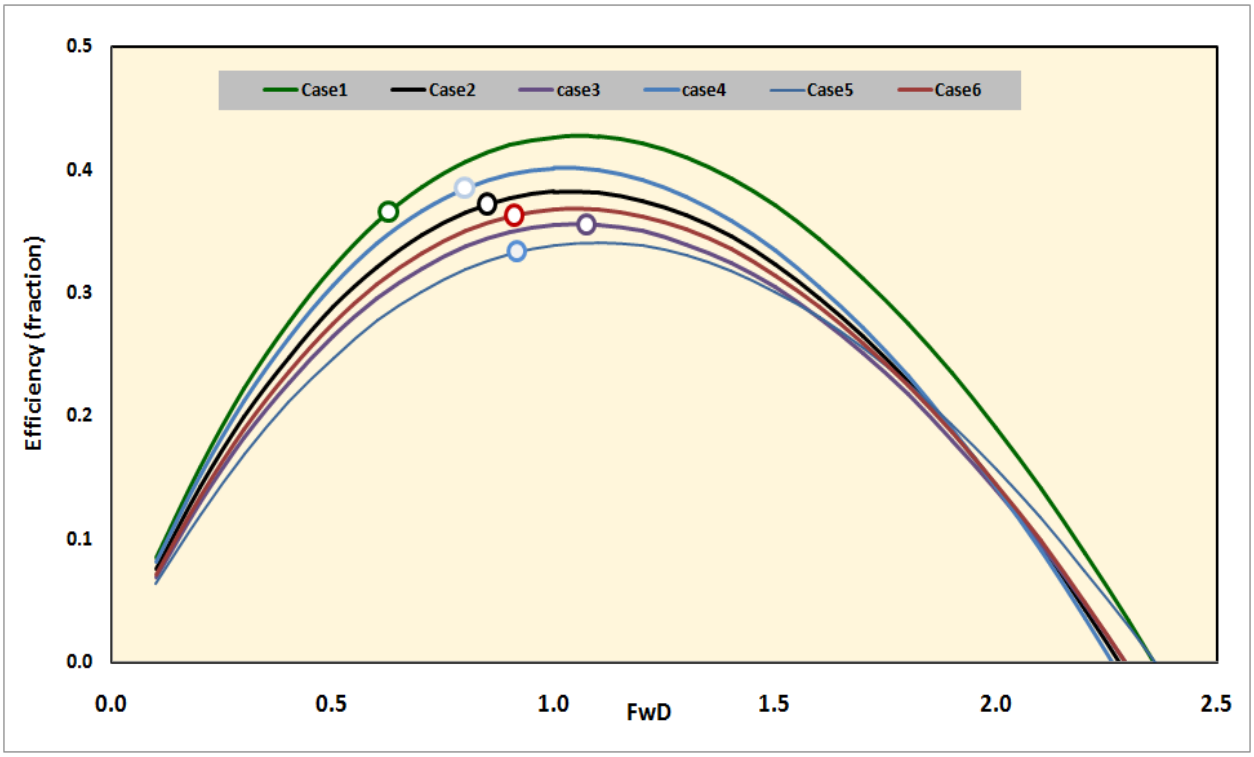

Fig. 15: Efficiency vs. F_{wd} for different cases

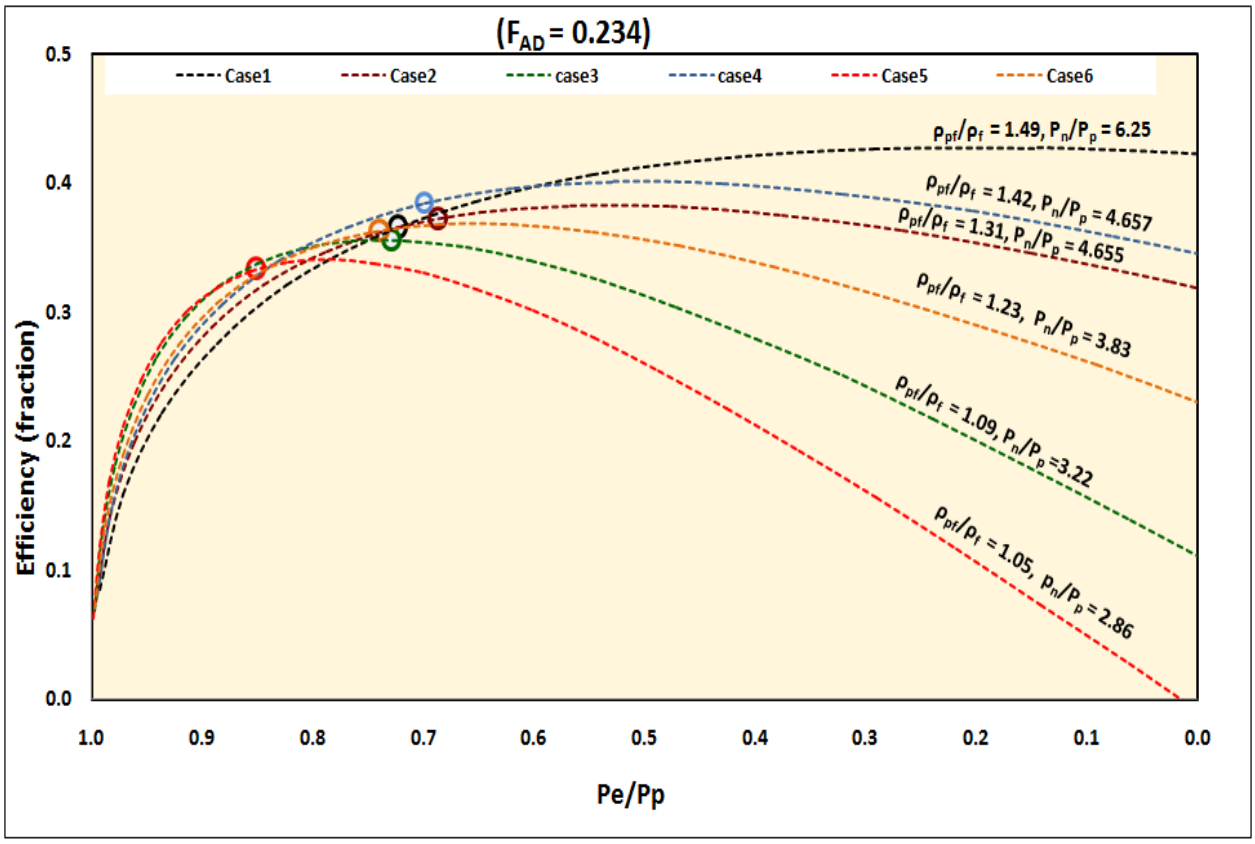

Fig. 16: Efficiency vs. P_e/P_p for different cases

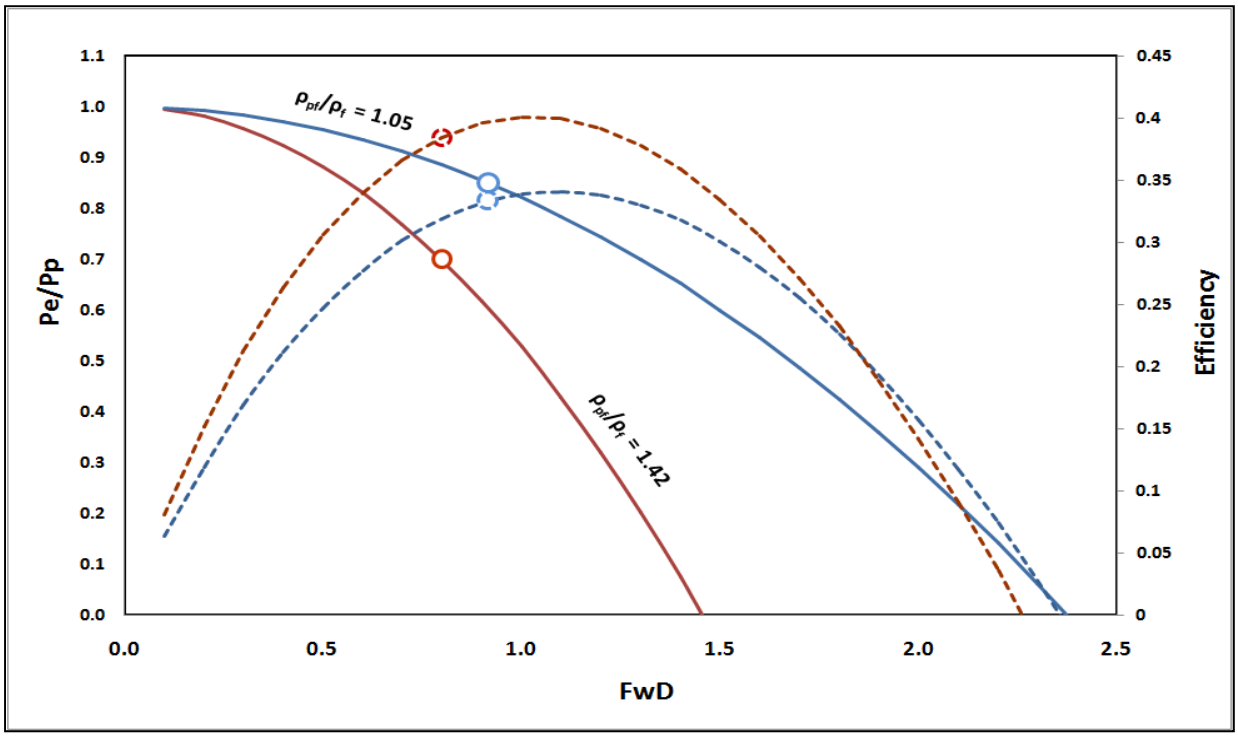

Fig. 17: Effect of P_e/P_p on efficiency and FwD

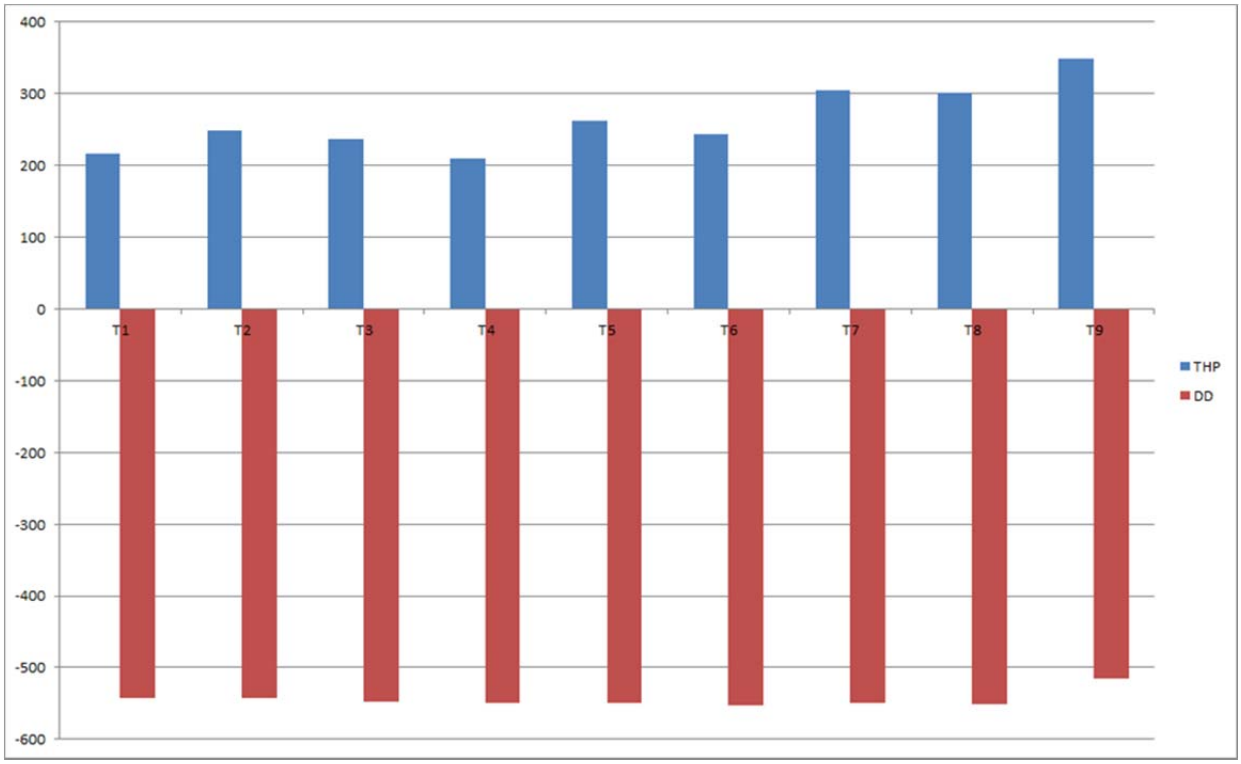

Fig. 18: Limited drawdown with a JP

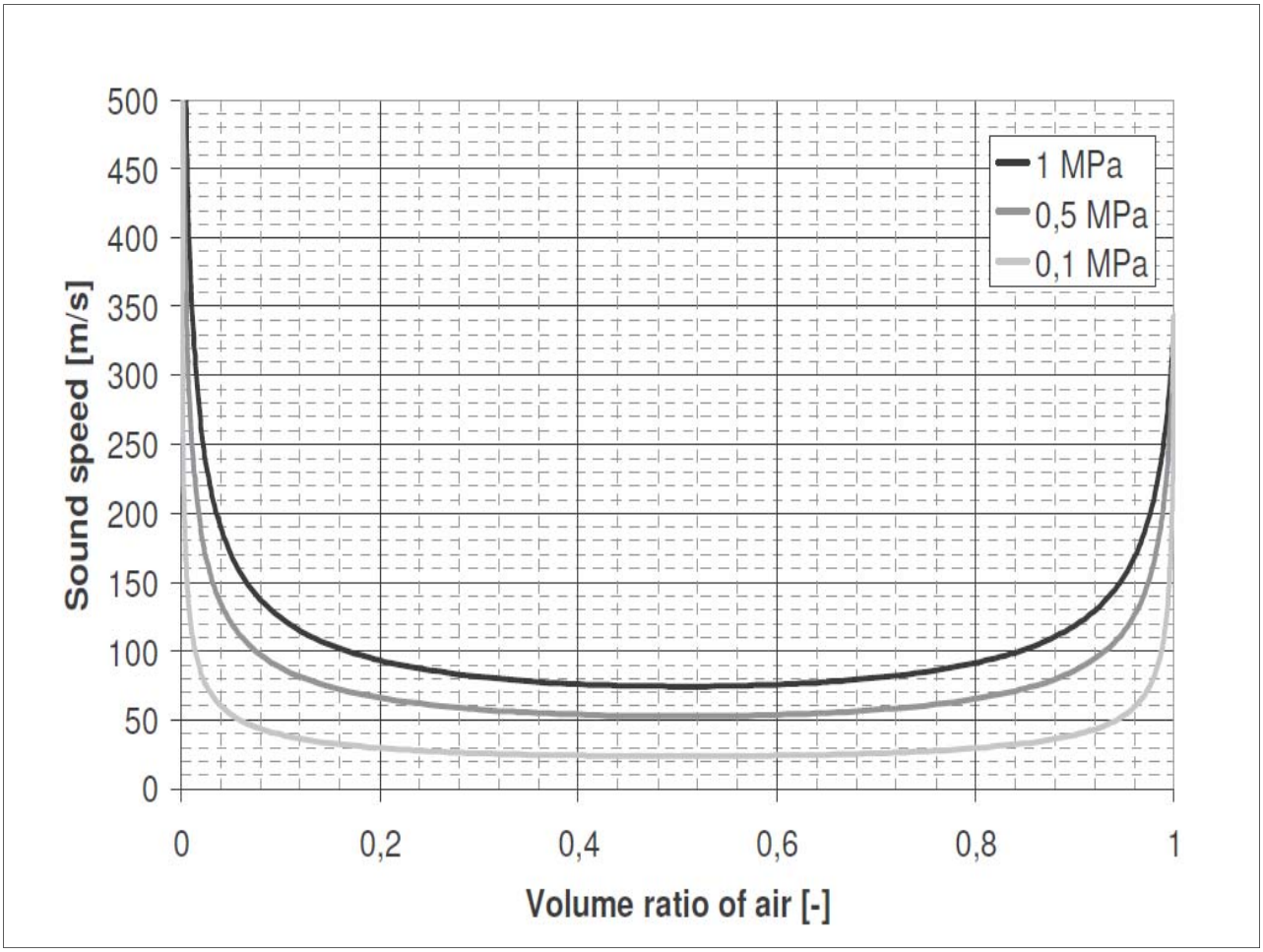

Fig. 19: Air/water mixture velocity (Courtesy: Daniel HIMR et al.)